J. Phys.: Condens. Matter **2** (1990) 187–194. Printed in the UK

Minimum energy versus metastable magnetisation processes in antiferromagnetically coupled ferromagnetic multilayers

B Dieny† and J P Gavigan
Laboratoire Louis Néel, CNRS, 166X, 38042 Grenoble Cédex, France

Received 8 September 1989, in final form 30 October 1989

Abstract. This paper reports calculations of magnetisation processes in antiferromagnetically coupled ferromagnetic multilayers of uniaxial or cubic in-plane anisotropy, for the hypothesis that the system always finds the state of absolute minimum energy. These calculations are complementary to those reported in our previous paper where the system followed the local energy minimum via coherent rotation of the magnetic moments. Both sets of calculations are used to discuss briefly experimentally measured magnetisation processes in a number of real systems as reported in the literature.

1. Introduction

Magnetic multilayers constitute model systems for the study of fundamental magnetism because they offer the possibility of tailoring sample properties according to pre-determined specifications. One example of this is the study of magnetisation processes in antiferromagnetically coupled multilayer systems where the interlayer coupling strength through the non-magnetic material is quite weak and where the resulting ratio of anisotropy energy to interlayer exchange energy lies in the range 10^{-2} to 10^{2}. The corresponding field values required to characterise the various transitions in the magnetisation process (spin flop, saturation, . . .) range up to 10^{-3}–10^{-1} T; these values are easily achieved experimentally. This is rather different to the case of bulk antiferromagnets where the corresponding ratio lies in the range 10^{-4} to 1 and where fields of 10 to 10^{3} T would be necessary to characterise magnetisation processes.

In the previous paper [1], we investigated magnetisation and demagnetisation processes in such highly idealised multilayer systems, consisting of ferromagnetic layers of uniaxial or cubic in-plane anisotropy with antiferromagnetic coupling between adjacent layers. Calculated magnetic phase diagrams, initial magnetisation curves and hysteresis loop shapes were reported for bilayers for all possible initial moment configurations with respect to applied field and for both easy and hard axis anisotropy. Scaling laws to deduce the magnetic behaviour of an infinite multilayer from the calculations for bilayers were also reported. In a number of particular cases, the effects of having a finite number of layers and boundaries on the calculated magnetic behaviour were investigated. The

† Present address: IBM Almaden Research Center, 650 Harry Road, K63/803 San Jose, CA 95120-6099, U.S.A.

0953-8984/90/010187 + 08 $03.50

scaling laws were found to hold for multilayers with more than thirty periods ($n = 30$), while in the particular case of spin flops, the transition field was found to be sensitive to the parity of n (i.e. odd or even). All these calculations were performed in the limiting case of coherent rotation of the magnetic moments where each layer was assumed to be single domain, the moments were constrained to lie in the film plane and the energy of the system followed the local energy minimum in which it initially found itself. This gave rise in many cases to quite large hysteresis and metastable symmetric and asymmetric moment configurations.

In real materials, however, magnetisation processes also involve the nucleation of domains and the propagation of domain walls. These mechanisms tend to drive the system to the state of absolute minimum energy. Thus, a second set of calculations can be performed for a second limiting situation in which it is assumed that through nucleation and propagation, the system always finds the configuration of absolute minimum energy. Such an energy state is single domain despite the dynamics and multi-domain processes involved in reaching it. Magnetisation curves calculated in this second limiting case never show hysteresis. Some such calculations were already reported in [2] but are presented in this paper in more detail together with all relevant phase diagrams and in such a way as to facilitate comparison between the two limiting situations. The value of such a study lies in its use in interpreting experimental hysteresis loops, given that the magnetisation processes must resemble to a greater or lesser extent one or other of the limiting mechanisms and in any case will lie somewhere between the two.

This second set of calculations were performed using the bilayer approximation as in [1]. The internal energy of a bilayer is given by

$$E = \cos(\theta_1 - \theta_2) - b(\cos\theta_1 + \cos\theta_2) + E_{A1} + E_{A2}$$

so the equilibrium moment configuration is determined by the coupled equations

$$\begin{aligned} \partial E/\partial\theta_1 = 0 &\Leftrightarrow -\sin(\theta_1 - \theta_2) + b\sin\theta_1 + \partial E_{A1}/\partial\theta_1 = 0 \\ \partial E/\partial\theta_2 = 0 &\Leftrightarrow +\sin(\theta_1 - \theta_2) + b\sin\theta_2 + \partial E_{A2}/\partial\theta_2 = 0 \end{aligned} \tag{1}$$

with the stability condition

$$(\delta^2 E/\partial\theta_1^2)\partial^2 E/\partial\theta_2^2 - (\partial^2 E/\partial\theta_1\partial\theta_2)^2 > 0.$$

E_A represents the in-plane anisotropy energy, θ_1 and θ_2 are the angular positions of the moments with respect to the applied field and the magnetic moments are of unit modulus. $E_A = k\cos^2\theta\sin^2\theta$ in the case of cubic anisotropy and $E_A = d\cos^2\theta$ in the case of uniaxial anisotropy. The lower case letters b, k and d indicate normalisation with respect to the strength of the antiferromagnetic coupling J_0 (i.e. $b = B/J_0$, $k = K/J_0$ and $d = D/J_0$). The absolute energy minimum was determined by choosing between all the local energy minima calculated for a given set of parameters.

2. Cubic in-plane anisotropy

Following the absolute energy minimum magnetisation processes necessarily gives rise to just one phase diagram for each case of positive and negative anisotropy (i.e. for the field applied along an easy or hard direction). This is contrary to the case of coherent rotation where a multitude of different situations arise depending on the initial state in which the system is prepared.

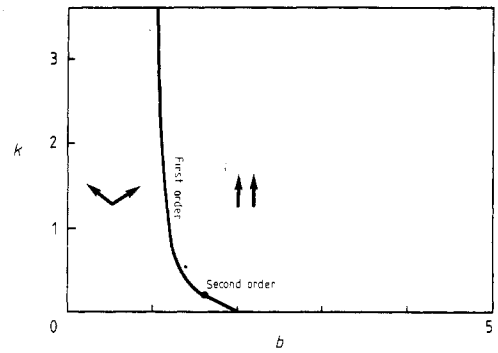

Figure 1. (k, b) magnetic phase diagram for the absolute minimum energy configuration in the case of $k > 0$ (cubic anisotropy). The curve traces the locus of b_{sat} (the field at which saturation is reached), as a function of k.

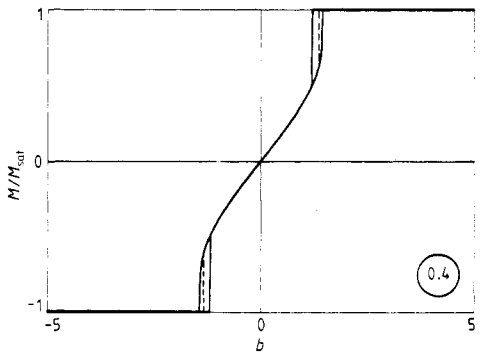

Figure 2. Minimum energy magnetisation curve (MEMC: broken line) and coherent rotation hysteresis loop (CRHL: full line) for $k = 0.4$.

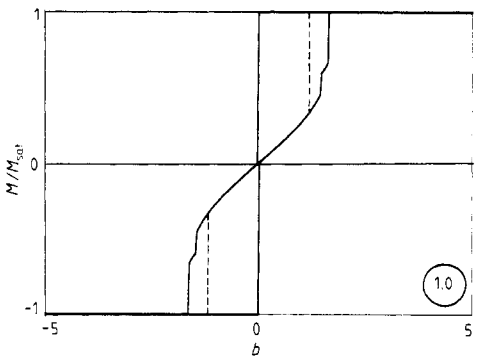

Figure 3. MEMC (broken line) and CRHL (full line) for $k = 1.0$.

2.1. $k > 0$

The relevant phase diagram for positive anisotropy is shown in figure 1. As is clear from the figure, the minimum energy state always corresponds to a symmetric moment configuration with respect to the applied field, which lies along an easy axis of magnetisation. No spin-flop or spin-flip transitions are expected. For $k < 0.2$, saturation is reached via a second-order transition at a field $b_{sat} = 2(1 - k)$. Above 0.2, saturation is reached via a first-order transition at a value b_{sat} given by the solution to the equations:

$$\begin{aligned} &-2\cos\theta + b + 2k\cos\theta\cos 2\theta = 0 \\ &1 - 2b = \cos 2\theta - 2b\cos\theta + (k/2)\sin^2 2\theta. \end{aligned} \tag{2}$$

Note that $\theta_1 = 2\pi - \theta_2 = \theta$ as the moments are symmetric about the field direction. The asymptotic expression for b_{sat} in the limit of large k is $b_{sat} = 1 + (2 + k)/[4(1 + k^2)]$.

2.1.1. Magnetisation curves. In figures 2 to 5, calculated magnetisation curves following the field dependence of the absolute energy minimum are traced together with the hysteresis loops calculated for the coherent rotation hypothesis [1]. The curves for $k < 0.2$ are not reported as they coincide for both hypotheses. Curves for the absolute energy minimum are shown by the broken lines. In general we can expect the real

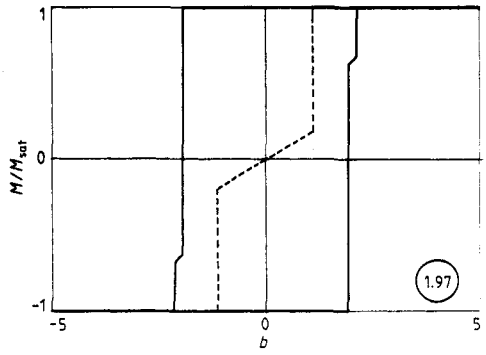

Figure 4. MEMC (broken line) and CRHL (full line) for $k = 1.97$.

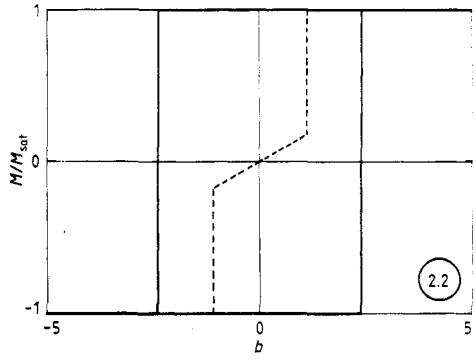

Figure 5. MEMC (broken line) and CRHL (full line) for $k = 2.2$.

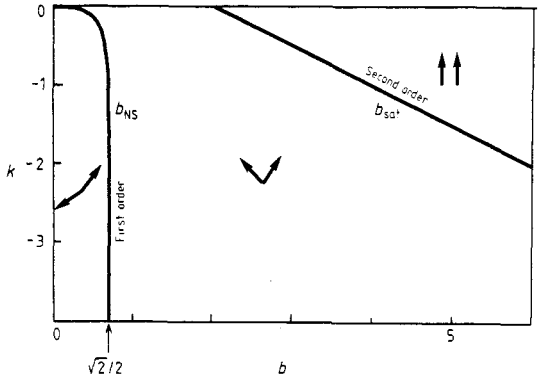

Figure 6. (k,b) magnetic phase diagram for the absolute minimum energy configuration in the case of $k < 0$ (cubic anisotropy). The curve on the left traces the locus of b_{NS} at which a first-order transition from a non-symmetric to a symmetric configuration occurs. The line on the right traces the locus of b_{sat}.

hysteresis loop to fall between the two limits. This would lead to a reduced amount of energy dissipated per cycle in cases of high anisotropy where the coherent rotation mechanism is likely to be less favoured due to its high instability with respect to the absolute minimum. In the case of $k = 0.4$, a significant proportion of the curves coincide about the origin. In such a case where there is no hysteresis, it is still possible to imagine that structural defects and inhomogeneities may resist either the coherent rotation or domain wall movement resulting in a finite amount of hysteresis about zero (see for example the case of Fe–Cr multilayers [3] discussed in section 4).

2.2. $k < 0$

Figure 6 shows the phase diagram for the state of absolute minimum energy when the field is applied along a hard direction. The features of this diagram are essentially the same as those in the corresponding case for coherent rotation (figure 11 in [1]). The main difference is that the first-order transition field b_{NS} from a non-symmetric to symmetric configuration occurs in progressively lower fields for $k < -0.14$ than in the

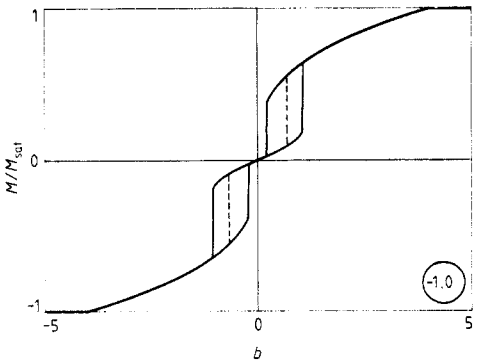

Figure 7. MEMC (broken line) and CRHL (full line) for $k = -1.0$.

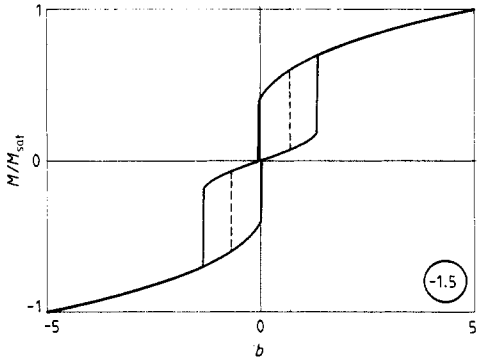

Figure 8. MEMC (broken line) and CRHL (full line) for $k = -1.5$.

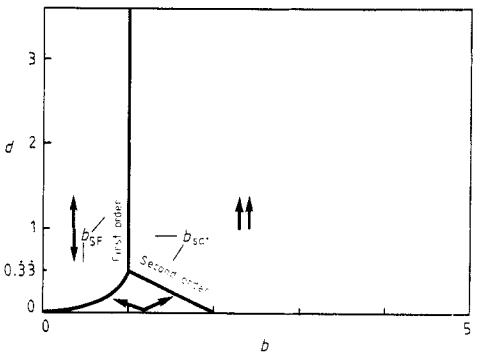

Figure 9. (d, b) magnetic phase diagram for the absolute minimum energy configuration in the case of $d > 0$ (uniaxial anisotropy). The b_{sf} curve indicates a spin-flop transition below $d = \frac{1}{3}$ and a spin-flip transition when $b_{SF} = b_{sat}$ for $d > \frac{1}{3}$.

case of coherent rotation. This critical line defining b_{NS} is determined by the solution of the following coupled equations:

$$\left.\begin{aligned}\partial E/\partial\theta_1 = 0 \Leftrightarrow -\sin(\theta_1-\theta_2)+b\sin\theta_1+(k/2)\sin 4\theta_1 = 0\\ \partial E/\partial\theta_2 = 0 \Leftrightarrow +\sin(\theta_1+\theta_2)+b\sin\theta_2+(k/2)\sin 4\theta_2 = 0\end{aligned}\right\}\ \text{non-symmetric configuration}$$

$$\partial E/\partial\theta = 0 \Leftrightarrow -2\cos\theta + b + 2k\cos\theta\cos 2\theta = 0 \quad \text{symmetric, i.e. } \theta_1 = 2\pi - \theta_2 = \theta$$

and

$$E(\theta_1, \theta_2) = E(\theta) \Leftrightarrow \cos(\theta_1 - \theta_2) - b(\cos\theta_1 + \cos\theta_2) + (k/4)(\sin^2 2\theta_1 + \sin^2 2\theta_2)$$

$$= \cos 2\theta - 2b\cos\theta + (k/2)\sin^2 2\theta.$$

It can be shown, for large k, that b reaches an asymptotic value equal to $(\sqrt{2})/2$. Saturation is reached via a second-order transition at $b_{sat} = 2(1 - k)$.

Figures 7 and 8 show the minimum energy curves with the corresponding coherent rotation hysteresis loops for two values of k (figure 18 of [1]). No example is shown for $k > -0.14$ for which the two situations are equivalent.

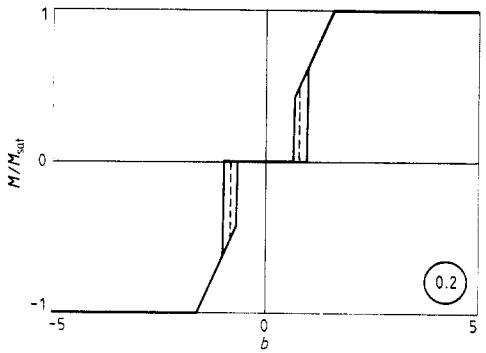

Figure 10. MEMC (broken line) and CRHL (full line) for $d = 0.2$.

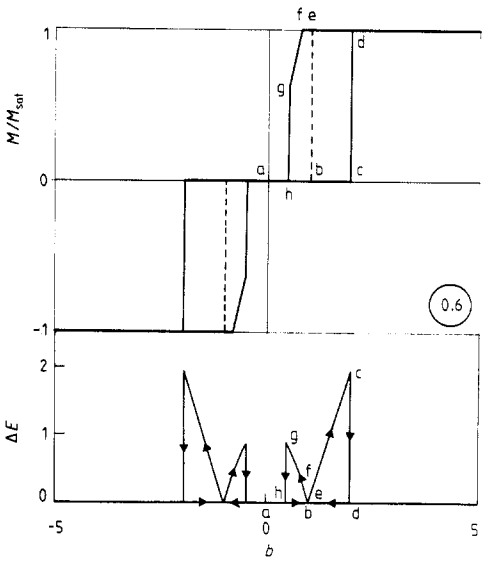

Figure 11. MEMC (broken line) and CRHL (full line) for $d = 0.6$. The lower part traces the energy difference between the MEMC and CRHL curves and represents the degree of instability of the coherent rotation configuration with respect to the absolute minimum energy state.

3. Uniaxial anisotropy

For uniaxial anisotropy, $d > 0$ (i.e. field applied parallel to the easy axis) is the only case considered here, as the $d < 0$ situation always leads to reversible behaviour [1].

The absolute minimum energy phase diagram is shown in figure 9 (compare figure 20 of [1]). Up to $d = \frac{1}{3}$, the magnetisation process involves a spin-flop transition followed by a progressive closing of the moments to saturation. The critical curves defining the spin flop and saturation are given by the equations $b = 2\sqrt{[d(1-d)]}$ and $b = 2(1-d)$. For $d > \frac{1}{3}$ saturation is reached directly via a spin-flip transition, which in the case of figure 9 occurs at $b_{SF} = 1$ and is independent of d.

Figures 10–13 show the minimum energy curves and hysteresis loops as in the cubic case. In the lower part of figure 11, the energy difference between the two limiting magnetisation curves is traced. Following the path a → b, the curves coincide and $\Delta E = 0$. Between b and c, as the curves diverge, there is a linear increase in energy of the metastable state with respect to the absolute minimum. This drops instantly to zero (c → d) as saturation is reached and the curves again coincide. Decreasing the field, coincidence remains until e is reached at which point ΔE begins increasing linearly to f and then parabolically to g, before again falling to zero at h. Such diagrams are qualitatively useful in predicting the magnetisation process for a real system. For example, the larger the metastability ΔE is, the greater will the tendency for the system to find a path to a lower energy state be. Thus in a real system, for the parameters for which the curves in figure 11 were calculated, the more one increases the field along the line b → c, the more likely will it be for the system to find a path to saturation intermediate between the two limiting extremes.

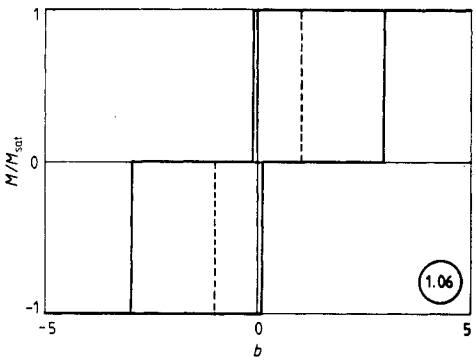

Figure 12. MEMC (broken line) and CRHL (full line) for $d = 1.06$.

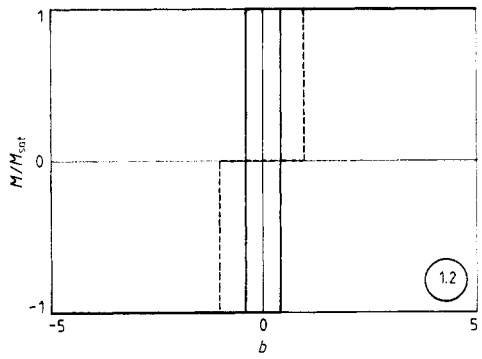

Figure 13. MEMC (broken line) and CRHL (full line) for $d = 1.2$.

4. Comparison with experimental data and conclusion

A number of papers have appeared recently in the literature that are specifically concerned with magnetisation processes in antiferromagnetically coupled magnetic multilayers and sandwiches, e.g. [Fe/Cr] [3–6] and [Co/Cu] [7]. In [7], analysis of [110] hard axis magnetisation curves for $[9Co/5Cu]_{103}$ and $[6Co/8Cu]_{62}$ multilayers gave values for k $(=K/J_0)$ of -3.57 and -2.28 respectively. Specific 'coherent rotation' calculations were reported in this paper also, taking into account the finite number of layers (see also [1]). It was found that these calculations agree with experimental data in the range of fields from positive saturation down to the coercive field. In stronger negative fields, the experimental data resemble more the curve of absolute energy minimum reported in this paper, plus some hysteresis with remanence due to complicated multidomain processes involving the nucleation of domains to give non-symmetrical states [7].

In [3], hard axis hysteresis loops were reported for several (100) [Fe/Cr] multilayers of varying periodicity and Cr thickness. Deduced values of anisotropy and exchange were also reported. For all the samples studied K/J_0 is of the order of 10^{-2} despite the decrease of J_0 with increasing Cr thickness. These low values of K/J_0 correspond to positions near the origin in the k versus b phase diagram, unlike in the case of the [Co/Cu] multilayers. The apparent variation of hysteresis loop shape with increasing Cr thickness should therefore disappear on plotting on a normalised field axis (B/J_0). In terms of the model, the unique loop shape should correspond to the limiting case for coherent rotation (see figures 7 and 8 and figure 18 of [1]). The occurrence, however, of a finite amount of hysteresis, as mentioned in section 2.1, is possibly due to retarded coherent rotation due to structural defects and inhomogeneities.

Grünberg *et al* [4–6] discuss in some detail magnetisation processes in epitaxial Fe–Cr–Fe sandwiches in which the Fe layers are antiferromagnetically coupled. In [5] they identify a spin-flop transition in low fields by magneto-optical methods, which corresponds to the coherent rotation calculation prediction (see figure 2 in [1]). They also report qualitatively different hysteresis loop shapes for respectively [110]- and [100]-type growth. Those for [100]-type growth resemble the curves reported in [3] for multilayers. The symmetry of [110]-type growth, however, leads to in-plane uniaxial anisotropy and not cubic. Thus, as the ratio $d = D/J_0$ is approximately the same as in

the multilayers, the [110] hysteresis loop resembles those of figures 10 and 11 calculated for uniaxial anisotropy.

To conclude, here we have given a few illustrative examples of the use of the calculations reported in this paper and in [1] and [2]. As the field of research on magnetic multilayers expands, these calculations will become more useful in characterising the magnetic properties of such novel systems and, in particular, their response to an externally applied magnetic field.

Acknowledgment

J P Gavigan is a post-doctoral research fellow of the Commission of the European Communities.

References

[1] Dieny B, Gavigan J P and Rebouillat J P 1990 *J. Phys.: Condens. Matter* **2** 159–85
[2] Dieny B, Gavigan J P and Rebouillat J P 1989 *Materials Research Society Symp. Proc.* vol 151, 35
[3] Nguyen Van Dau F, Fert A, Etienne P, Baibich M N, Broto J P, Chazelas J, Creuzet G, Frederich A, Hadjoudi S, Hurdequint H, Redoules J P and Massies J 1988 *J. Physique Coll.* **49** C8 1633
[4] Grünberg P *Proc. 12th Int. Coll. Magnetic Films and Surfaces* (1988, *Le Creusot, France*) unpublished
[5] Grünberg P, Schreiber R, Pang Y, Brodsky M P and Sowers H 1988 *Phys. Rev. Lett.* **57** 2442
[6] Saurenbach F, Walz U, Hinchey H, Grünberg P and Zinn W 1988 *J. Appl. Phys.* **63** 3473
[7] Rebouillat J P, Fillion G, Dieny B, Cebollada A, Gallego J M and Martinez J L 1989 *Materials Research Society Symp. Proc.* vol 151, 117